electronics MDPI

Communication

Resistive Switching Characteristic of Cu Electrode-Based RRAM Device

Huanmei Yuan [1,2,*], Tianqing Wan [3] and Hao Bai [1]

[1] School of Metallurgical and Ecological Engineering, University of Science and Technology Beijing, Beijing 100083, China
[2] Department of Electronic & Computer Engineering, Hong Kong University of Science & Technology, Kowloon, Hong Kong 999077, China
[3] Department of Applied Physics, Hong Kong Polytechnic University, Kowloon, Hong Kong 999077, China
* Correspondence: yuanhuanmei@ustb.edu.cn

Abstract: The conductive bridge random access memory (CBRAM) device has been widely studied as a promising candidate for next-generation nonvolatile memory applications, where Cu as an electrode plays an important role in the resistive switching (RS) process. However, most studies only use Cu as one electrode, either the top electrode (TE) or the bottom electrode (BE); it is rarely reported that Cu is used as both TE and BE at the same time. In this study, we fabricated CBRAM devices by using Cu as both the TE and BE, and studied the RS characteristic of these devices. With Al_2O_3 as the switching layer (5~15 nm), the devices showed good bipolar RS characteristics. The endurance of the device could be as high as 10^6 cycles and the retention time could be as long as 10^4 s. The Al_2O_3 thickness influences the bipolar RS characteristic of the devices including the initial resistance, the forming process, endurance, and retention performance. The Cu electrode-based RRAM devices also present negative bias-suppressed complementary resistive switching (CRS) characteristics, which makes it effective to prevent the sneak path current or crosstalk problem in high-density memory array circuits.

Keywords: bipolar RS characteristic; Al_2O_3 switching layer; Cu electrode; CBRAM; CRS

Citation: Yuan, H.; Wan, T.; Bai, H. Resistive Switching Characteristic of Cu Electrode-Based RRAM Device. *Electronics* **2023**, *12*, 1471. https://doi.org/10.3390/electronics12061471

Academic Editor: Dongseok Suh

Received: 20 February 2023
Revised: 14 March 2023
Accepted: 15 March 2023
Published: 20 March 2023

Copyright: © 2023 by the authors. Licensee MDPI, Basel, Switzerland. This article is an open access article distributed under the terms and conditions of the Creative Commons Attribution (CC BY) license (https://creativecommons.org/licenses/by/4.0/).

1. Introduction

Resistive switching random access memory (RRAM) provides attractive prospects for next-generation non-volatile memories due to its outstanding characteristics, high memory capacity, simple structure, excellent scalability and compatibility with the standard complementary metal oxide semiconductor (CMOS) process [1–3]. Typically, the RRAM device shows a metal–insulator–metal (MIM) structure, where an insulator (oxide) material is simply sandwiched between the metal top electrode (TE) and bottom electrode (BE). With this structure, metal electrodes have a great influence on the resistive switching (RS) characteristics of RRAM devices [4,5]. So far, various kinds of metal electrodes have been studied for RRAM devices with RS behavior, such as Cu, Pt, TiN, Ag, Al, W, Ti, etc. [6–11]. Herein, Cu is an important electrode material in conductive bridge random access memory (CBRAM) as it can supply metal ions into a switching layer (SL) to form a metal conductive filament (CF). Li et al. [12] indicated that RRAM devices with Cu TE exhibited more stable bipolar RS behavior compared with Au and Al. Yang et al. [13] investigated the reset switching of bipolar $Cu/HfO_2/Pt$ RRAM devices with a statistical methodology, and they determined that the ON state resistance (R_{ON}) describing the initial state of the CF has considerable influence on the distributions of the reset current and voltage. Until now, there have been many studies on RRAM devices with Cu electrodes, such as Ag/ZnO/Cu [8], $Cu/AlO_x/W$ [9], $Cu/HfO_2/Pt$ [10], etc. However, most of these studies only use Cu as either the TE or the BE, and very few studies address the topic of RS characteristics with Cu as both the TE and BE in the device. For the formation mechanism, a filamentary

switching mechanism has been proposed to explain the RS characteristic of CBRAM [14–18], where the conductive filament formation can be ideally explained by the electrochemical metallization model [19], i.e., when a positive voltage is applied on the oxidizable Cu electrode, the generated Cu^{+} or Cu^{2+} ions will migrate through the electrolyte onto the inert cathode and then will be reduced to Cu atoms at the cathode, leading to the CF growth from the cathode towards the anode. The mechanism of the CF rupture is more complicated, usually involving the oxidation of CF under the reverse electrical field and the dissolution of CF by the Joule heat [15,19–21]. However, whether the electrochemical oxidation or the thermal dissolution dominates the reset is still unaddressed.

In this study, we investigated the RS characteristics of RRAM devices with Cu as both the TE and BE, which helps to further explore the CF formation and rupture mechanism of Cu-based RRAM devices. In the meantime, the study on the RS characteristics of RRAM with Cu as both TE and BE is important for the wide application of RRAM. By utilizing Al_2O_3 as the SL material, we also studied the effect of SL thickness on the RS characteristics.

2. Materials and Methods

The RRAM devices with Cu as both TE and BE were fabricated as follows: first, a 60 nm Cu layer was successively deposited by direct current (DC) sputtering onto the low-resistivity silicon wafer (0.001~0.005 Ω·cm) to form the BE. Then, the SL of Al_2O_3 with a certain thickness (5~15 nm) was deposited by atomic layer deposition (ALD) at 300 °C. Finally, square-shaped Cu TEs (60 nm) with areas of $100 \times 100\ \mu m^2$ were deposited by DC sputtering through a lift-off process. Agilent B1500A semiconductor parameter analyzer was used to measure the RS characteristics with the bias voltage applied on the TEs while the BE was grounded.

3. Results

Figure 1 shows the structure diagram of the Cu electrode-based RRAM device. In this study, different kinds of RRAM devices ($Cu/Al_2O_3/Cu$ devices with the Al_2O_3 thickness of 5 nm, 10 nm, and 15 nm) were fabricated to study the effect of SL thickness on the RS characteristic of Cu electrode-based RRAM device. For the $Cu/Al_2O_3/Cu$ RRAM, the initial resistance of devices with 5 nm, 10 nm and 15 nm Al_2O_3 was tested at 12.8 MΩ, 17.7 MΩ and 51.9 MΩ, respectively, as shown in Figure 1b, which indicates an initial high resistance state (HRS). To trigger the resistive switching behaviour of these devices, a forming process with large voltage was conducted, and the results are shown in Figure 1c. The forming voltage used for devices with 5 nm, 10 nm, and 15 nm Al_2O_3 are 6 V, 8 V, and 9 V with the compliance current of 100 µA, 300 µA, and 500 µA, respectively. Therefore, the SL thickness obviously influences the performance of the RRAM device. With the increase in SL thickness, the initial resistance of the device increases, resulting in a larger forming voltage and compliance current. In any cases, once the RRAM device undergoes the forming process, it is easy to achieve the RS behaviour with a small voltage. Figure 1d shows the RS characteristic of the three devices. Under the compliance current of 500 µA, the set processes that the RRAM changes from HRS to low resistance state (LRS) occurred at 4 V, 4 V, and 3 V for devices with 5 nm, 10 nm, and 15 nm Al_2O_3, respectively. When the negative voltage was applied, a reset process (from LRS to HRS) occurred for these devices, where the on/off ratio can be estimated at approximately 86, 880, and 5388, and thus it can be roughly judged that CF formed in 15 nm Al_2O_3 is thicker than those formed in 10 nm and 5 nm under current conditions.

The on/off ratio is related to the testing parameters, and by properly adjusting the applied voltage or compliance current, the $Cu/Al_2O_3/Cu$ devices can achieve multi-level states. Taking the device with 10 nm Al_2O_3 as an example, as shown in Figure 2a, it can be seen that by increasing the voltage from 4 V to 5 V as well as the compliance current from 0.5 mA to 10 mA, the on/off ratio increases from 880 to almost 20,000, which is important for its applications. Under suitable testing parameters, we tested the endurance of these devices in the SPGU module of B1500A with the SET pulse (4 V, 200 ns) and RESET

pulse (−3 V, 200 ns) respectively, and the results are shown in Figure 2b–d. Compared with the Cu/Al_2O_3/Cu devices with 10 nm or 15 nm Al_2O_3. The device with 5 nm Al_2O_3 presented larger fluctuation in its HRS and LRS during the cycles. In any cases, all three Cu/Al_2O_3/Cu devices showed good endurance since their HRS and LRS showed stable trends in up to 10^6 cycles. In addition, the retention performances of these devices were also tested by applying a small voltage of 0.1 V on the HRS or LRS, and the results are shown in Figure 3. All the devices were tested for up to 10^4 s. During the process, the device with 5 nm Al_2O_3 showed obvious fluctuations in its HRS, but it was better in its LRS. For comparison, the devices with 10 nm or 15 nm Al_2O_3 showed more stable retention performance in both HRS and LRS. Therefore, Cu electrode-based RRAM devices with thicker Al_2O_3 layers tended to have better endurance and retention performance in this study.

In addition to the above bipolar RS characteristic, the Cu electrode-based RRAM devices also showed special RS behaviours during the testing process, as shown in Figure 4a–c. For this RS characteristic, the set and reset processes were finished in positive bias, and the devices kept in HRS within the whole negative bias, which is important in crossbar array application as it can prevent the sneak path current during the process (Figure 4d). Assume that when a read voltage (V_{read}) is applied to the RRAM of HRS, theoretically, there should be a small current (I_{read}) flowing along the black solid line path; however, in fact, there is I_{sneak} flowing along the red dotted line path. As a result, RRAM-a as originally HRS is misread as LRS. The special RS behaviours in Figure 4a–c can address this problem effectively. Take the Cu/(15 nm)Al_2O_3/Cu with a positive voltage as an example. The set process occurred (from HRS to LRS) at 2.28 V under the compliance current of 500 μA; then, when the voltage decreased back to 0.96 V, the reset process occurred (from LRS to HRS). However, the device keeps HRS when a negative voltage is applied, which is called negative bias suppression. Therefore, when it is applied to the crossbar array, any sneak path current involving the negative bias is blocked. It should be noted that the LRS only exists in a specific voltage range in this case, such as 0.96~4 V in the device of 15 nm Al_2O_3, which is similar to the complementary resistance switching (CRS) RRAM [22], while the simple structure and fabrication process of this device make it preferred in various applications.

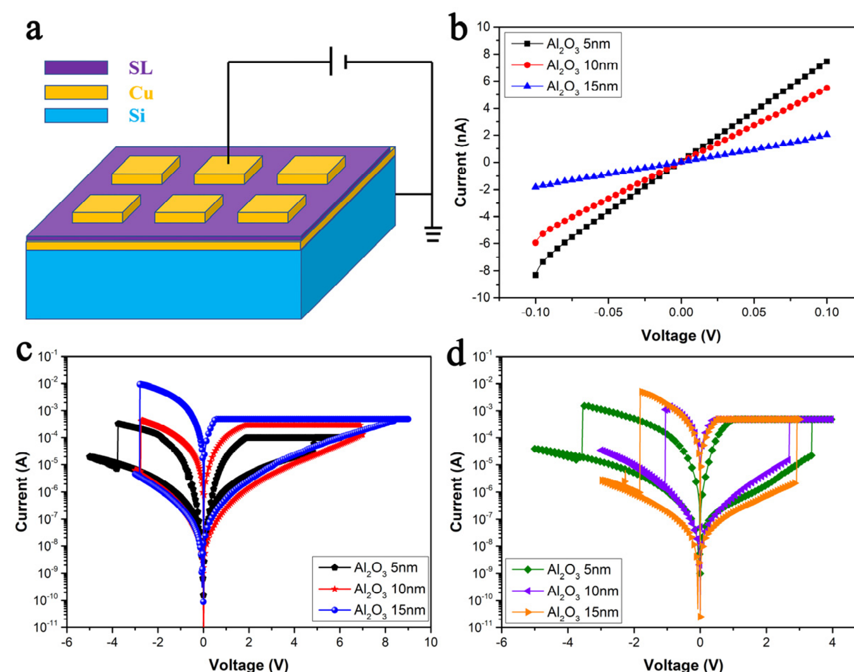

Figure 1. The structure diagram (**a**) of the Cu electrode-based RRAM device. The initial resistance (**b**), forming process (**c**), and RS behaviour (**d**) of the Cu/Al_2O_3/Cu devices with 5 nm, 10 nm, and 15 nm Al_2O_3.

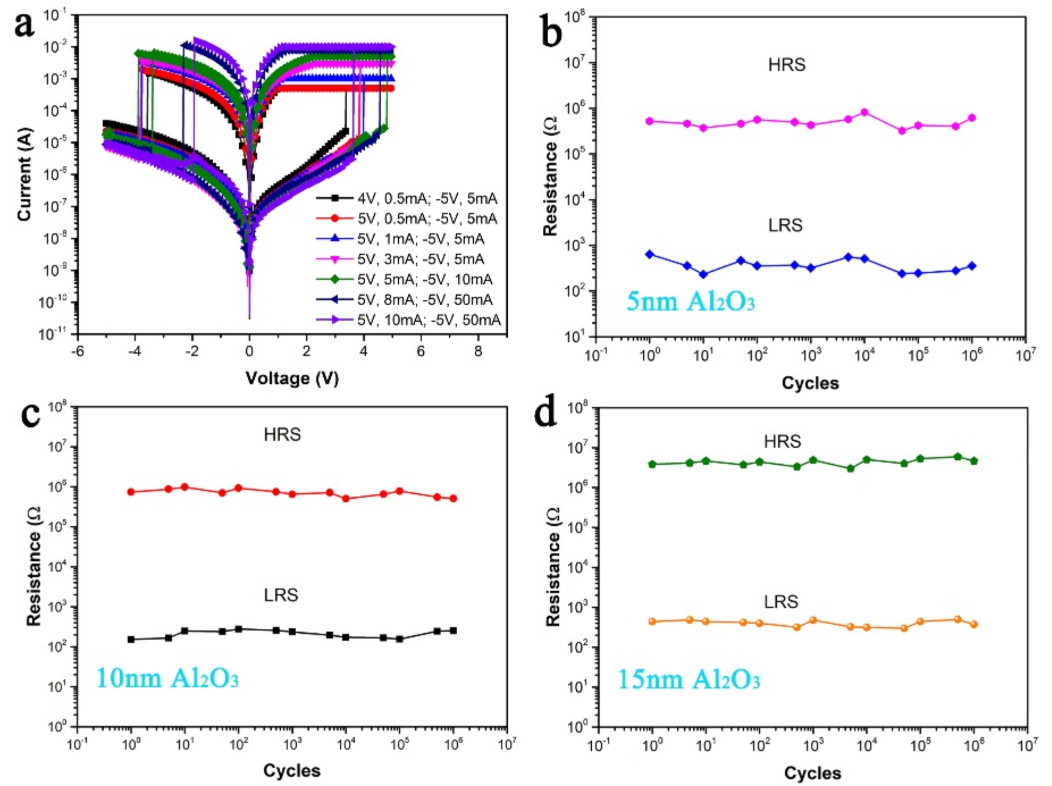

Figure 2. The multi-level state (**a**) of the Cu/Al_2O_3 (10 nm)/Cu devices. The endurance of devices with 5 nm (**b**), 10 nm (**c**), and 15 nm (**d**) Al_2O_3.

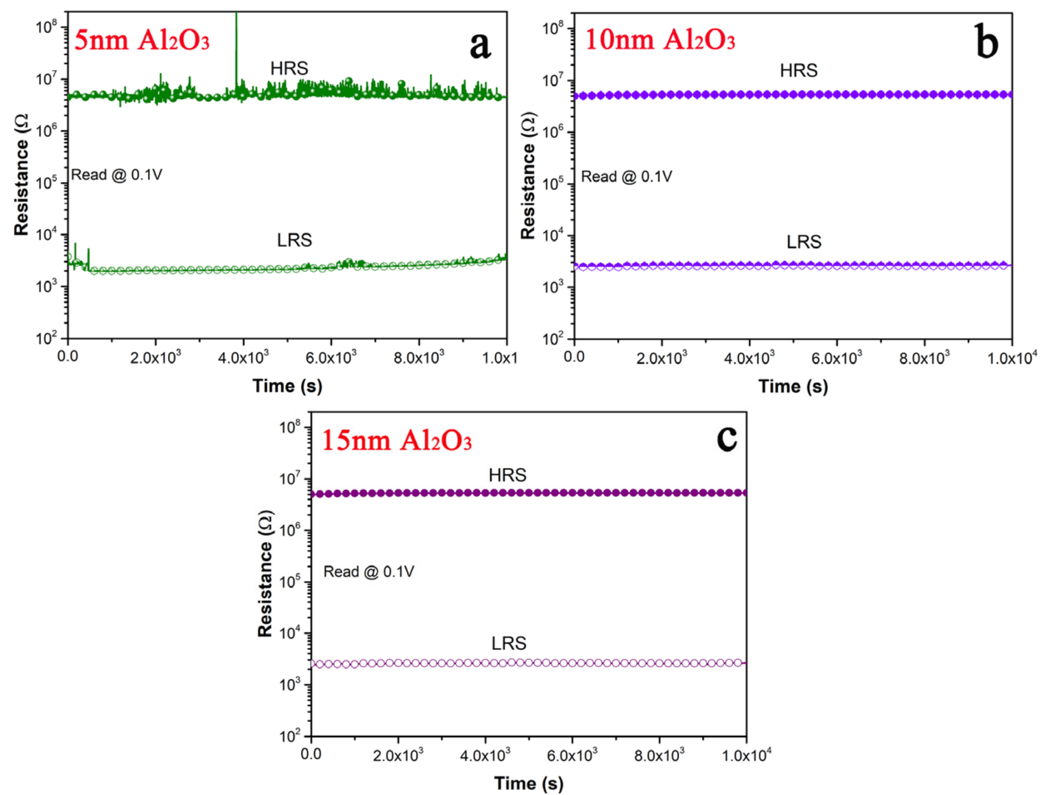

Figure 3. The retention of devices with 5 nm (**a**), 10 nm (**b**), and 15 nm (**c**) Al_2O_3.

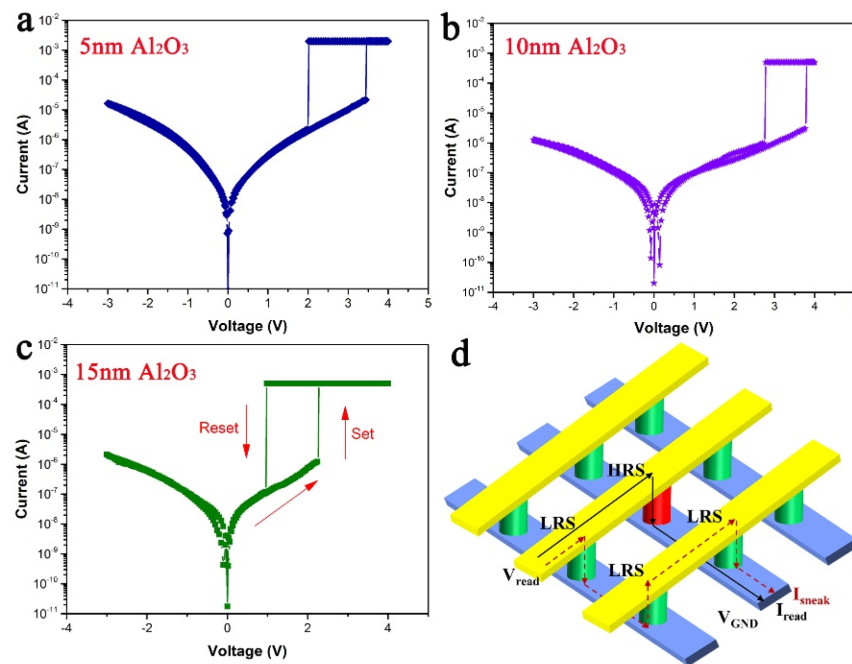

Figure 4. The negative bias-suppressed CRS characteristic of devices with 5 nm (**a**), 10 nm (**b**) and 15 nm (**c**) Al_2O_3. The sneak path current problem in the crossbar array (**d**).

4. Formation Mechanism of the Bipolar RS Characteristic

Based on the filamentary switching mechanism of the electrochemical metallization model [15,19–21], the mechanism of formation of the bipolar RS characteristic can be explained, as shown in Figure 5. Under the positive voltage (+V), Cu atoms in the TE are oxidized and converted into Cu ions. These Cu ions then drift from TE to BE with the electric field. During the process, some of these Cu ions are trapped at defect sites, meanwhile they are combined with the electrons from BE to form Cu atoms [10]. With the increase in positive voltage, more and more Cu ions are trapped and form Cu atoms. When the voltage increases to V_{set}, the trapped Cu atoms form a CF connecting the TE and BE, and the RRAM changes from HRS to LRS; that is the set process. When the negative voltage is applied, Cu^{2+} is formed in BE, which is drifted from BE to TE, and then neutralized by electrons from the TE. During the process, a high current is flowing through the filament with a large compliance current. When the voltage increases to V_{reset}, Joule heating/localized thermal heating caused by the high current [11] leads to the rupture of CF and the device changes from LRS to HRS; that is the reset process. However, further research is needed to study the negative bias-suppressed CRS characteristic in the device to control it and make it play a valuable role in various applications.

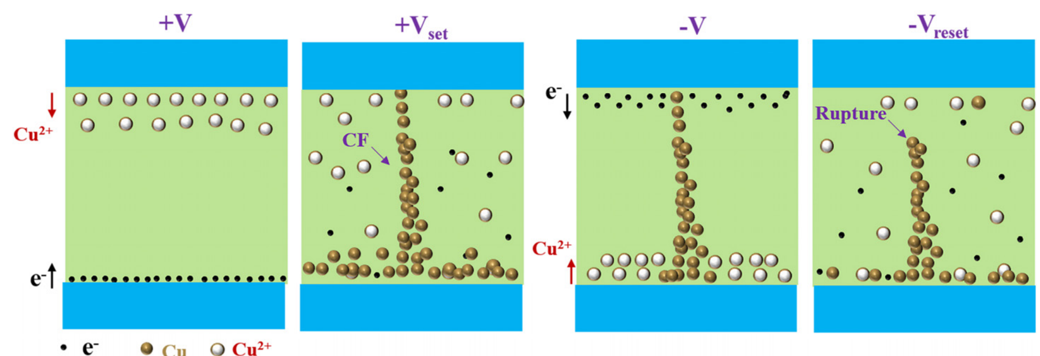

Figure 5. Schematic formation mechanism of the bipolar RS characteristic of the $Cu/Al_2O_3/Cu$ devices.

5. Conclusions

The RS characteristic of Cu electrode-based RRAM devices was studied in this work. Results demonstrated that the RRAM devices showed good bipolar RS characteristics, and by adjusting the applied voltage or compliance current, the devices presented a multi-level state with an on/off ratio as high as 20,000. The endurance test indicated that the devices can be stable for up to 10^6 cycles, and the retention test showed that the resistance kept at HRS (or LRS) for up to 10^4 s with little fluctuation under the read voltage of 0.1 V. With the increase in Al_2O_3 thickness from 5 nm to 15 nm, the initial resistance of the devices increases from 12.8 MΩ to 51.9 MΩ, thus requiring the forming voltage from 6 V to 9 V. In addition, the smaller thickness may make the resistance more fluctuating during the endurance and retention test. Most importantly, the Cu electrode-based RRAM devices also showed negative bias-suppressed CRS characteristic, which can prevent the sneak path current in the crossbar array applications. Finally, the mechanism of formation of the bipolar RS characteristic was explained, while further study is needed for the negative bias-suppressed CRS characteristic. Overall, the results presented in this work provide valuable information for establishing high-performance-based RRAM devices.

Author Contributions: H.Y., conceptualization, methodology, software, formal analysis, investigation, data curation and writing—original draft preparation; T.W., experimental operation and analysis; H.B., writing—review and editing, supervision, project administration. All authors have read and agreed to the published version of the manuscript.

Funding: This work was supported by the Hong Kong Scholars Program (XJ2020058).

Institutional Review Board Statement: Not applicable.

Informed Consent Statement: Not applicable.

Data Availability Statement: No new data were created or analyzed in this study. Data sharing is not applicable to this article.

Acknowledgments: We acknowledge the Nanosystem Fabrication Facility in Hong Kong University of Science and Technology for the fabrication service including the equipment and technical help.

Conflicts of Interest: We declare that we have no financial and personal relationships with other people or organizations that can inappropriately influence our work, there is no professional or other personal interest of any nature or kind in any product, service and/or company that could be construed as influencing the position presented in the research.

References

1. Jeon, K.; Kim, J.; Ryu, J.J.; Yoo, S.-J.; Song, C.; Yang, M.K.; Jeong, D.S.; Kim, G.H. Self-rectifying resistive memory in passive crossbar arrays. *Nat. Commun.* **2021**, *12*, 1–15. [CrossRef]
2. Li, Y.; Yin, L.; Wu, Z.; Li, X.; Song, X.; Gao, X.; Fu, L. Improved resistive switching uniformity of SiO_2 electrolyte-based resistive random access memory device with Cu oxidizable electrode. *IEEE Electron Device Lett.* **2019**, *40*, 1599–1601. [CrossRef]
3. Zhou, J.; Cai, F.; Wang, Q.; Chen, B.; Gaba, S.; Lu, W.D. Very low-programming-current RRAM with self-rectifying characteristics. *IEEE Electron Device Lett.* **2016**, *37*, 404–407. [CrossRef]
4. Hong, S.M.; Kim, H.-D.; An, H.-M.; Kim, T.G. Effect of work function difference between top and bottom electrodes on the resistive switching properties of SiN films. *IEEE Electron Device Lett.* **2013**, *34*, 1181–1183. [CrossRef]
5. Ye, C.; Wu, J.; He, G.; Zhang, J.; Deng, T.; He, P.; Wang, H. Physical mechanism and performance factors of metal oxide based resistive switching memory: A review. *J. Mater. Sci. Technol.* **2016**, *32*, 1–11. [CrossRef]
6. Arun, N.; Nageswara Rao, S.; Pathak, A. Effects of Bottom Electrode Materials on the Resistive Switching Characteristics of HfO2-Based RRAM Devices. *J. Electron. Mater.* **2022**, *52*, 1541–1551. [CrossRef]
7. Lin, C.-Y.; Wu, C.-Y.; Wu, C.-Y.; Hu, C.; Tseng, T.-Y. Bistable resistive switching in Al2O3 memory thin films. *J. Electrochem. Soc.* **2007**, *154*, G189. [CrossRef]
8. Muhammad, N.M.; Duraisamy, N.; Rahman, K.; Dang, H.W.; Jo, J.; Choi, K.H. Fabrication of printed memory device having zinc-oxide active nano-layer and investigation of resistive switching. *Curr. Appl. Phys.* **2013**, *13*, 90–96. [CrossRef]
9. Sleiman, A.; Sayers, P.; Mabrook, M. Mechanism of resistive switching in Cu/AlOx/W nonvolatile memory structures. *J. Appl. Phys.* **2013**, *113*, 164506. [CrossRef]
10. Tan, T.; Guo, T.; Chen, X.; Li, X.; Liu, Z. Impacts of Au-doping on the performance of Cu/HfO2/Pt RRAM devices. *Appl. Surf. Sci.* **2014**, *317*, 982–985. [CrossRef]

11. Zhao, J.; Chen, Q.; Zhao, X.; Yang, G.; Ma, G.; Wang, H. Self-compliance and high-performance GeTe-based CBRAM with Cu electrode. *Microelectron. J.* **2023**, *131*, 105649. [CrossRef]
12. Li, M.; Zhuge, F.; Zhu, X.; Yin, K.; Wang, J.; Liu, Y.; He, C.; Chen, B.; Li, R. Nonvolatile resistive switching in metal/La-doped BiFeO3/Pt sandwiches. *Nanotechnology* **2010**, *21*. [CrossRef]
13. Yang, X.; Long, S.; Zhang, K.; Liu, X.; Wang, G.; Lian, X.; Liu, Q.; Lv, H.; Wang, M.; Xie, H. Investigation on the RESET switching mechanism of bipolar Cu/HfO2/Pt RRAM devices with a statistical methodology. *J. Phys. D Appl. Phys.* **2013**, *46*, 245107. [CrossRef]
14. Guan, W.; Long, S.; Liu, Q.; Liu, M.; Wang, W. Nonpolar Nonvolatile Resistive Switching in Cu Doped ZrO_2. *IEEE Electron Device Lett.* **2008**, *29*, 434–437. [CrossRef]
15. Guan, W.; Ming, L.; Long, S.; Qi, L.; Wei, W. On the resistive switching mechanisms of Cu/ZrO_2:Cu/Pt. *Appl. Phys. Lett.* **2008**, *93*, 1625. [CrossRef]
16. Kim, K.M.; Jeong, D.S.; Hwang, C.S. Nanofilamentary resistive switching in binary oxide system; a review on the present status and outlook. *Nanotechnology* **2011**, *22*, 254002. [CrossRef] [PubMed]
17. Liu, Q.; Long, S.; Lv, H.; Wang, W.; Niu, J.; Huo, Z.; Chen, J.; Liu, M. Controllable growth of nanoscale conductive filaments in solid-electrolyte-based ReRAM by using a metal nanocrystal covered bottom electrode. *Acs Nano* **2010**, *4*, 6162–6168. [CrossRef] [PubMed]
18. Liu, Q.; Sun, J.; Lv, H.; Long, S.; Yin, K.; Wan, N.; Li, Y.; Sun, L.; Liu, M. Real-time observation on dynamic growth/dissolution of conductive filaments in oxide-electrolyte-based ReRAM. *Adv. Mater.* **2012**, *24*, 1844–1849. [CrossRef]
19. Waser, R.; Dittmann, R.; Staikov, G.; Szot, K. Redox-based Resistive Switching Memories—Nanoionic Mechanisms, Prospects, and Challenges. *Adv. Mater.* **2009**, *21*, 2632–2663. [CrossRef]
20. Yu, S.; Wong, H. A Phenomenological Model for the Reset Mechanism of Metal Oxide RRAM. *IEEE Electron Device Lett.* **2010**, *31*, 1455–1457. [CrossRef]
21. Zhou, P.; Li, Y.; Sun, Q.Q.; Lin, C.; Ding, S.J.; Jiang, A.Q.; Zhang, D.W. The Temperature Dependence in Nanoresistive Switching of HfAlO. *IEEE Trans. Nanotechnol.* **2012**, *11*, 1059–1062. [CrossRef]
22. Chai, Y.; Wu, Y.; Takei, K.; Chen, H.-Y.; Yu, S.; Chan, P.C.; Javey, A.; Wong, H.-S.P. Nanoscale bipolar and complementary resistive switching memory based on amorphous carbon. *IEEE Trans. Electron Devices* **2011**, *58*, 3933–3939. [CrossRef]

Disclaimer/Publisher's Note: The statements, opinions and data contained in all publications are solely those of the individual author(s) and contributor(s) and not of MDPI and/or the editor(s). MDPI and/or the editor(s) disclaim responsibility for any injury to people or property resulting from any ideas, methods, instructions or products referred to in the content.